

peak in the total pion-production cross section. We therefore feel that it is quite important for another experiment to verify this effect.

We would like to thank the entire ZGS staff for their support and encouragement throughout the experiment. We would also like to thank Dr. J. G. Asbury, Professor A. L. Read, and Dr. M. T. Lin for their help in the early stages of this experiment, and Mr. P. Kalbaci for his help in running it.

*Work supported by a research grant from the U. S. Atomic Energy Commission and carried out at the Argonne National Laboratory zero-gradient synchrotron.

¹L. G. Ratner, K. W. Edwards, C. W. Akerlof, D. G.

Crabb, J. L. Day, A. D. Krisch, and M. T. Lin, *Phys. Rev.* **166**, 1353 (1968).

²D. G. Crabb, J. L. Day, A. D. Krisch, M. T. Lin, M. L. Marshak, J. G. Asbury, L. G. Ratner, and A. L. Read, *Phys. Rev. Letters* **21**, 830 (1968).

³W. F. Baker *et al.*, *Phys. Rev. Letters* **7**, 101 (1961); R. A. Lundy, T. B. Novey, D. D. Yovanovitch, and V. L. Telegdi, *Phys. Rev. Letters* **14**, 504 (1965); A. N. Diddens *et al.*, *Nuovo Cimento* **31**, 961 (1964); D. Deckers *et al.*, *Phys. Rev.* **137**, B962 (1965); E. W. Anderson *et al.*, *Phys. Rev. Letters* **19**, 198 (1967); J. V. Allaby *et al.*, in *Proceedings of the Fourteenth International Conference on High Energy Physics*, Vienna, Austria, 1968 (unpublished).

⁴The target-empty effect was still about 25%. The production cross section decreased when we looked at negative angles. The Cherenkov pressure curves were completely flat over several hundred lb/in.².

PHOTOPRODUCTION OF CHARGED PION PAIRS ON PROTONS

H. Alvensleben, U. Becker, William K. Bertram, M. Chen, K. J. Cohen, T. M. Knasel, R. Marshall, D. J. Quinn, M. Rohde, G. H. Sanders, H. Schubel, and Samuel C. C. Ting
Deutsches Elektronen-Synchrotron, Hamburg, Germany, and Department of Physics and
Laboratory for Nuclear Science, Massachusetts Institute of Technology, Cambridge, Massachusetts
(Received 22 September 1969)

A high-statistics (100 000 events) measurement of photoproduction of charged pion pairs on protons is reported in two parts. First, the measured cross sections are presented in a three-dimensional data matrix where all the dynamical features are explicitly shown. Second, fitting the data in the energy region 2.6–6.8 GeV with various assumptions on ρ production indicates that $d\sigma/dt|_{t=0}$ for the photoproduction of ρ decreases with increasing energy similar to πN scattering.

We report an experiment on the reaction

$$\gamma p \rightarrow p \pi^+ \pi^- \quad (1)$$

at forward production angles, with incident energy between 2.6 and 6.8 GeV and in the di-pion mass (m) region from 500 to 1000 MeV/ c^2 .^{1,2} With a total of 100 000 events, cross sections were measured at energy intervals of $\Delta E_\gamma = 0.6$ GeV and at mass intervals of $\Delta m = 30$ MeV/ c^2 .

The purposes of this experiment are (1) to study the detailed production mechanism of pion pairs without any theoretical assumptions by making an accurate measurement of the di-pion spectrum as a function of both mass and energy; and (2) to study the energy dependence of the forward ρ -production cross section by simultaneously fitting various assumptions for the ρ -production mechanism, mass, width, and a general background in m and p to the extensive data.

This measurement of the production cross section differs markedly from most previous measurements where one is limited by statistics or

where the ρ cross sections were obtained from the measured $\pi\pi$ spectrum by assuming zero background.

The experiment.—This experiment was done at the DESY 7.5-GeV electron synchrotron using a bremsstrahlung beam with an average intensity of 3×10^{10} equivalent quanta/sec, a 60-cm H₂ target, and a pair spectrometer similar to the one described previously.³ Two threshold Cherenkov counters in the system separated electrons from pions; protons were rejected by time of flight. During the experiment, magnetic fields were kept constant to 3 parts in 10^4 and counter voltages to ± 5 V. Every 4 h a normalization run was made on ρ production with a carbon target and the system was found to be reproducible to $\pm 1\%$ during the entire period of running.

The 22 500 hodoscope combinations in the magnetic spectrometer defined a mass resolution of $\Delta m/m = \pm 1.7\%$, and a momentum resolution of $\Delta p/p = \pm 3.0\%$. The beam intensity was controlled such that the dead-time corrections were $\leq 2\%$

and the accidentals, measured from coincidence circuits of different resolving times, were $\leq 1\%$. Corrections were made for beam attenuation in the H_2 target, empty-target effects, and absorption via nuclear interactions in the H_2 target, in the target cell, in the scintillation counters, and in the Cherenkov counters.^{4,5}

Many experimental checks were made to ensure that the spectrometer behaved as designed and that all corrections were understood. For example, the effects of nuclear absorption of π pairs by the Cherenkov counters were investigated by measuring the π absorption rate as a function of the pressure in the counters. The relative change of $\pi\pi$ yields was found to be in agreement with calculations based on published π -nucleus data.⁴ To reduce possible systematic effects due to the bremsstrahlung beam, all the spectra were taken with $k_{\max}/p \cong 1.15$. k_{\max} is the peak bremsstrahlung energy, and p is the central spectrometer momentum.

The acceptance was calculated by a Monte Carlo method. A sufficient number of Monte Carlo events was generated so that the errors in the measured cross sections are due only to experimental statistics and small systematic uncertainties. Essential to the Monte Carlo integration was the accurate determination of the magnet-transport equations. Because of the accuracy needed, neither first- nor second-order transport theory could be used. Instead, the equations were determined by numerically integrating a family of 80 trajectories through a grid of the measured field values of each magnet. The transport coefficients were then obtained from the trajectories by a least-squares method. The

transport equations included all terms linear, bilinear, and pure quadratic in x, x', z, z' , and $\delta p_0/p_0$ (except those excluded by symmetry) and terms up to fourth order in $(\delta p_0/p_0)/(1 + \delta p_0/p_0)$. Trajectories obtained from these coefficients agreed in position and angle to 3 parts in 10^3 with those obtained from exact numerical integration. The effects of multiple scattering and of π decay in flight along the spectrometer were also considered in the Monte Carlo calculation.

The data.—Figure 1(a) shows the data in three dimensions with the measured experimental cross sections⁶ displayed as a function of the variables m and p . [Table I shows the numerical values of the points in Fig. 1(a).] These data enable direct comparison with various models in a straightforward way. Two principal features appear in Fig. 1(a): (1) The spectra are dominated by the ρ ; and (2) for every mass bin from 500 to 1000 MeV/ c^2 the spectrum exhibits a p dependence of the type $d^2\sigma/d\Omega dm \sim p^2(1 + R/p)^2$ with $R > 0$, rather than a p^2 dependence. This behavior shows that the forward $\pi\pi$ production cross section $d^2\sigma/dtdm$ decreases with increasing energy, similar to the case of πN scattering. Figure 1(b) shows some typical projected mass bins as functions of p .

The analysis.—The analysis of Reaction (1) in terms of ρ production is complicated because there is no theory for wide resonances and the form of the background is not known. It is for these reasons that we have presented the experimental data in Table I without any theoretical assumptions. To analyze our data we have fitted the cross sections of Table I with the following equations:

$$d^2\sigma/d\Omega dm = Cg(p)[2mR(m)(m_p/m)^4] + f_{BG}(p, m), \quad (2)$$

$$d^2\sigma/d\Omega dm = Cg(p)[2mR(m) + I(m)] + f_{BG}(p, m), \quad (3)$$

$$d^2\sigma/d\Omega dm = Cg(p)\{2mR(m)(m_p/m)^4 + I(m)\} + f_{BG}(p, m), \quad (4)$$

with

$$R(m) = \frac{1}{\pi} \frac{m_p \Gamma_\rho(m)}{(m_p^2 - m^2)^2 + m_p^2 \Gamma_\rho^2(m)}, \quad \Gamma_\rho(m) = \frac{m_\rho}{m} \left[\frac{(\frac{1}{2}m)^2 - m_\pi^2}{(\frac{1}{2}m_p)^2 - m_\pi^2} \right]^{3/2} \Gamma_0,$$

$$g(p) = p^2 \left(1 + \frac{R}{p} \right)^2, \quad I(m) = A \frac{m^2 - m_p^2}{(m_p^2 - m^2)^2 + m_p^2 \Gamma_\rho^2(m)},$$

$$f_{BG}(p, m) = \left(\sum_{i=1}^4 a_i p^{i-1} \right) \left(\sum_{j=1}^4 b_j m^{j-1} \right) \geq 0;$$

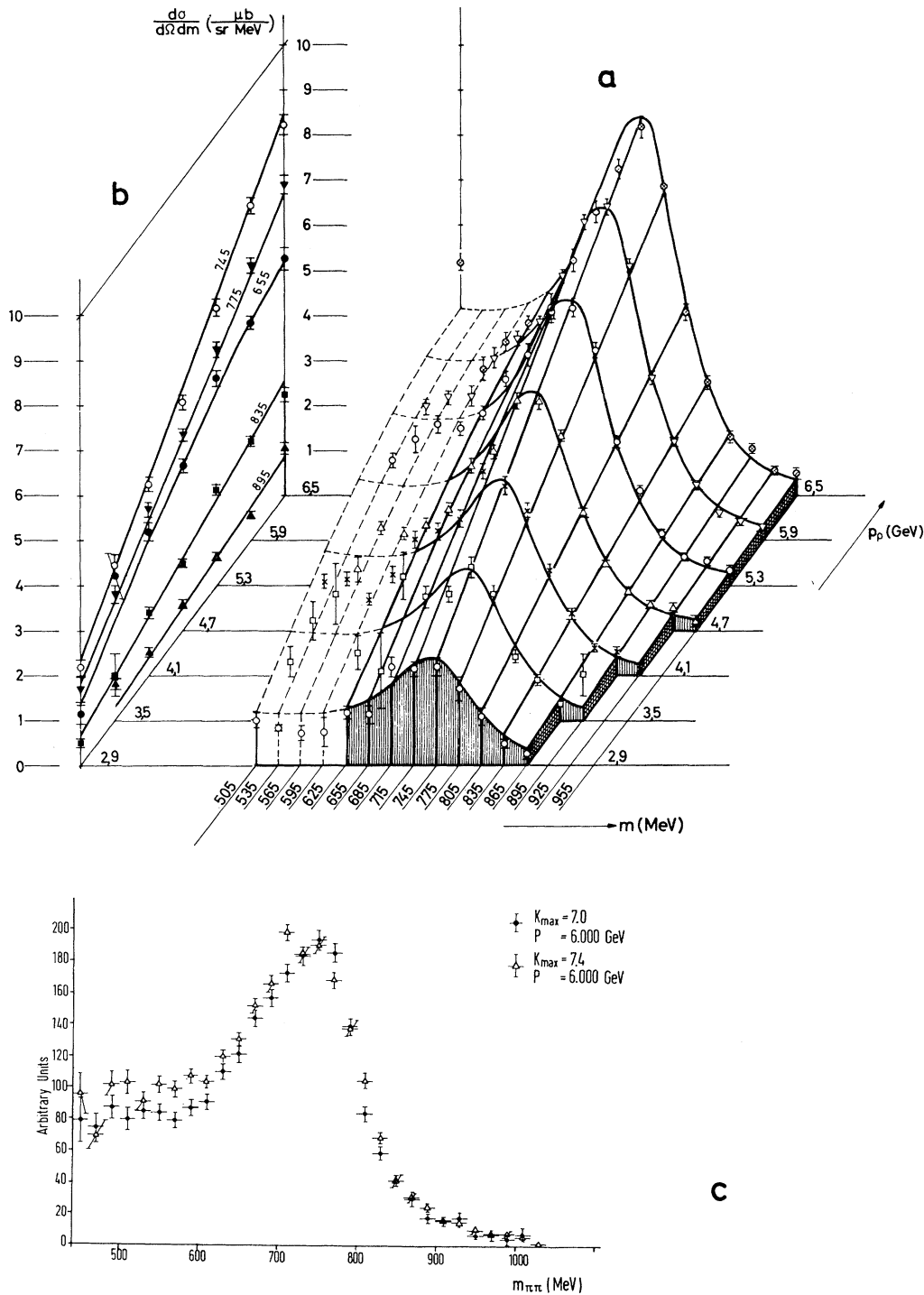


FIG. 1. (a) Experimentally measured cross sections $d^2\sigma/d\Omega dm$ in $\mu\text{b}/(\text{sr MeV}/c^2)$ of Reaction (1) as a function of the variables m and p . The curves are best fits by Eq. (2) (the background is not shown). Similar curves were obtained for fits by Eqs. (3) and (4). (b) Projections of (a) onto the $(p, d^2\sigma/d\Omega dm)$ plane for fixed values of m . The curves are best fits by $d^2\sigma/d\Omega dm = p^2(1 + R/p)^2$. This shows explicitly that the data for fixed m increase more slowly than p^2 ($R > 0$). (c) Comparison of mass spectra for different peak bremsstrahlung energy with the same central spectrometer momentum. The agreement of the spectra above 610 MeV/ c^2 indicates that the inelastic contribution to the spectra above this mass is small.

Table I. Data matrix, $d^2\sigma/d\Omega dm$ in $\mu\text{b}/(\text{sr MeV}/c^2)$ as function of p (GeV/ c), the total laboratory momentum of the di-pions, and m (in MeV/ c^2), the invariant mass of the pion pair.

$m \backslash p$	6.5	5.9	5.3	4.7	4.1	3.5	2.9
955	.51 \pm .13	.29 \pm .06	.38 \pm .12	.25 \pm .11			
925	.57 \pm .10	.42 \pm .08	.55 \pm .10	.52 \pm .11	.17 \pm .12		
895	1.06 \pm .11	.59 \pm .08	.64 \pm .09	.60 \pm .09	.53 \pm .11	1.02 \pm .48	
865	1.32 \pm .14	1.24 \pm .09	1.16 \pm .10	.87 \pm .09	.62 \pm .09	.38 \pm .09	.26 \pm .13
835	2.55 \pm .16	2.20 \pm .11	2.11 \pm .12	1.48 \pm .09	1.39 \pm .13	.92 \pm .12	.49 \pm .10
805	4.08 \pm .19	3.62 \pm .15	3.20 \pm .14	2.63 \pm .11	2.34 \pm .14	1.43 \pm .15	1.09 \pm .20
775	6.86 \pm .21	6.09 \pm .17	5.23 \pm .18	4.33 \pm .13	3.67 \pm .16	2.80 \pm .19	1.70 \pm .29
745	8.21 \pm .25	7.42 \pm .18	6.17 \pm .20	5.07 \pm .17	4.24 \pm .16	3.42 \pm .23	2.17 \pm .20
715	7.26 \pm .22	7.07 \pm .17	6.08 \pm .18	5.11 \pm .19	4.54 \pm .18	2.79 \pm .19	2.14 \pm .15
685	6.29 \pm .23	5.85 \pm .17	5.45 \pm .17	3.96 \pm .17	3.47 \pm .20	2.73 \pm .25	2.17 \pm .22
655	5.23 \pm .25	4.84 \pm .15	4.59 \pm .18	3.65 \pm .16	3.19 \pm .20	3.20 \pm .51	1.13 \pm .21
625	4.18 \pm .32	4.50 \pm .16	3.84 \pm .17	2.68 \pm .15	3.02 \pm .19	1.08 \pm .85	1.17 \pm .14
595	3.13 \pm .25	4.05 \pm .23	3.49 \pm .16	2.34 \pm .14	2.23 \pm .18	1.49 \pm .38	.73 \pm .33
565	3.44 \pm .21	3.21 \pm .22	3.56 \pm .20	2.15 \pm .13	1.67 \pm .14	2.78 \pm .69	.70 \pm .18
535	2.82 \pm .26	3.17 \pm .15	3.24 \pm .30	2.26 \pm .15	2.12 \pm .15	2.21 \pm .44	.81 \pm .09
505	5.17 \pm .80	2.96 \pm .17	2.77 \pm .18	1.33 \pm .28	2.07 \pm .16	1.28 \pm .34	.95 \pm .17

$g(p)$ is the energy dependence of the forward-production cross section—if $g(p)=p^2$ ($R=0$), we have the classical diffraction scattering with a constant total cross section. With $g(p)=p^2(1+R/p)^2$ and $R > 0$, $(d\sigma/dt)|_{t=0}$ decreases with increasing ρ energy. The background function $f_{BG}(m, p)$ is the product of two general third-order polynomials in m and p . The function $I(m)$ (the Soeding term)⁷ represents an interference of the ρ amplitude with a part of the background, where the nonresonant photoproduced pairs are diffractively produced off the nucleon. $R(m)$ and $\Gamma_\rho(m)$ are the relativistic p -wave resonance formulas proposed by Jackson.⁸

Equation (2) represents the fitting of the $\pi\pi$ cross section by a ρ -production term where the resonance formula is modified by a phenomenological "Ross-Stodolsky" term⁹ $(m_\rho/m)^4$ plus a general background. The factor $(m_\rho/m)^4$ also appears in a model by Kramer and Uretsky⁹ and has been used at DESY and Stanford Linear Accelerator Center to account for the shifts and shape distortion of the photoproduced ρ spectrum. Equation (3) represents another commonly accepted procedure to fit the spectrum with the mass shift and shape distortion accounted for by an interference term $I(m)$, whose magnitude (A) is determined by the fit. Equation (4) assumes both mechanisms can be present.

Fitting was done in two ways. First, each of Eqs. (2)-(4) was fitted to the data of Table I using

the CERN fitting program MINUIT.¹⁰ The following quantities were free parameters in the fits: a_i , b_j , C , m_ρ , Γ_0 , R , and A . A lower cutoff limit, m_0 , used in fitting the data was chosen in the following way: Figure 1(c) shows two mass spectra from 460 to 1000 MeV/ c^2 . One was taken with a peak bremsstrahlung energy at 7.4 GeV and the other at 7.0 GeV. Both had a central spectrometer momentum of 6.0 GeV/ c . Since, as seen, the two spectra are in agreement above 610 MeV/ c^2 one concludes that the inelastic contribution above this mass is small. The same result was found for spectra at $k_{\text{max}} = 5.55$ and 5.25 GeV. Therefore m_0 was chosen to be 610 MeV/ c^2 . Checks were made by varying $610 < m_0 < 760$ MeV/ c^2 ; the values of m_ρ , Γ_0 , C , R , A , and the background function were found to be insensitive to these changes. Studies were also made on the background function $f_{BG}(m, p)$ and it was found that the results of a product of second-order polynomials were consistent with those of the higher order function described above. The values of m_ρ and Γ_0 obtained from all fits done in this manner were consistent with $m_\rho = 765 \pm 10$ MeV/ c^2 and $\Gamma_0 = 145 \pm 10$ MeV/ c^2 .

Second, using the values $m_\rho = 765$ MeV/ c^2 and $\Gamma_0 = 145$ MeV/ c^2 obtained above, the mass spectrum for each momentum was fitted separately by Eqs. (2)-(4). In this way both the cross sections and the background were left with an arbitrary momentum dependence, in contrast to the first

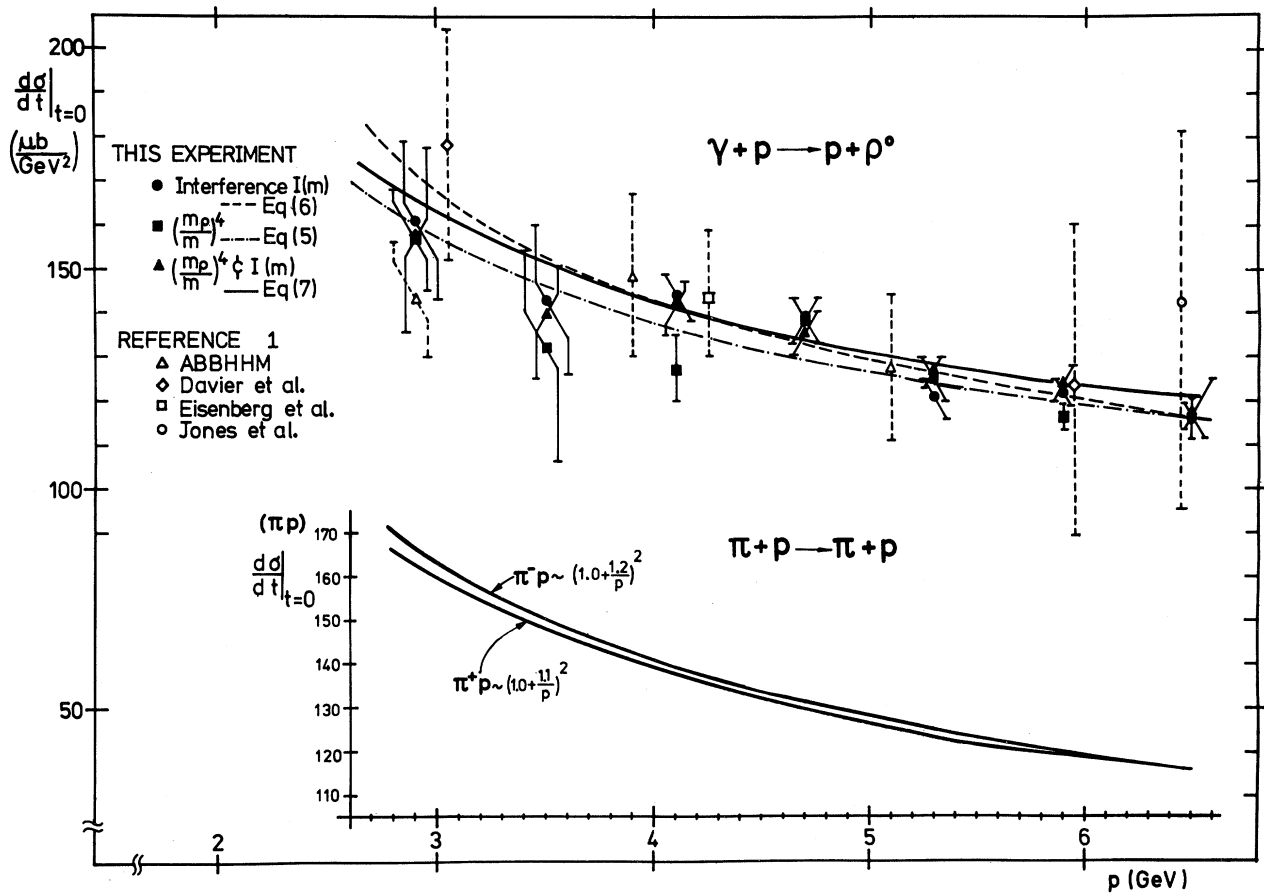


FIG. 2. Comparison with other experiments and results of our measurements obtained by fitting the data matrix (Table I) with Eqs. (2)-(4). Also shown is a comparison of the best fits to our cross sections as a function of p and the πN cross section as a function of p normalized to the same scale.

method, where both the cross section and the background were required to be smooth functions of the momentum. The results of these fits were found to be insensitive within the limits of $m_\rho = 765 \pm 10 \text{ MeV}/c^2$ and $\Gamma_\rho = 145 \pm 10 \text{ MeV}/c^2$ quoted above. Figure 2 shows the values of $d\sigma/dt|_{t=0}$ obtained in this way,¹¹ and they are seen to be insensitive to assumptions (2), (3), or (4). Figure 2 also includes the results of other experiments in the same energy region. As seen, these data are in good agreement with the present experiment. (The counter data from Cornell² are not shown since they were analyzed without any subtraction of background, and with a fixed width of $120 \text{ MeV}/c^2$, in contrast to the values of $145 \text{ MeV}/c^2$ determined by us and by the bubble-chamber groups.)

From these fits the following was observed:

(1) By fitting $d\sigma/dt|_{t=0}$ to a p dependence of the form $(1 + R/p)^2$, the following results were obtained:

(a) $d\sigma/dt|_{t=0}$ from fits to Eq. (2) (Ross-Stodolsky factor) yields

$$\frac{d\sigma}{dt}|_{t=0} \sim \left(1 + \frac{1.0 \pm 0.3}{p}\right)^2. \quad (5)$$

(b) $d\sigma/dt|_{t=0}$ from fits to Eq. (3) (interference) yields

$$\frac{d\sigma}{dt}|_{t=0} \sim \left(1 + \frac{1.3 \pm 0.3}{p}\right)^2. \quad (6)$$

(c) $d\sigma/dt|_{t=0}$ from fits to Eq. (4) (both Ross-Stodolsky factor and interference) yields

$$\frac{d\sigma}{dt}|_{t=0} \sim \left(1 + \frac{1.0 \pm 0.4}{p}\right)^2. \quad (7)$$

This is to be compared with the momentum dependence of π^+p and π^-p cross sections in the en-

ergy region from 3.0 to 7.0 GeV,⁵

$$\left. \frac{d\sigma}{dt} \right|_{t=0} \sim \sigma_{\pi^+\rho}^2 (1 + \alpha_+^2) \sim \left(1 + \frac{1.1 \pm 0.1}{p} \right)^2,$$

$$\left. \frac{d\sigma}{dt} \right|_{t=0} \sim \sigma_{\pi^-\rho}^2 (1 + \alpha_-^2) \sim \left(1 + \frac{1.2 \pm 0.1}{p} \right)^2.$$

p is in GeV/ c and α_{\pm} = (Real part)/(Imaginary part) for $\pi^{\pm}p$ scattering. Therefore, independent of our assumption, the energy behavior of ρ production is found to be very similar to πN scattering in the same energy region.

(2) The mass of the rho we measured from $\rho \rightarrow \pi^+\pi^-$ is about the same as measured by $\rho \rightarrow e^+e^-$, but the width of the rho is about 30 MeV/ c^2 higher.¹²

(3) With our measured value¹² of $\gamma_{\rho}^2/4\pi = 0.45 \pm 0.10$ and the best-fit value of $d\sigma/dt|_{t=0}$ at 6.0 GeV one obtains a $\sigma_{\rho N}$ of 24 ± 3 mb.

We are grateful for the support of Professor W. Jentschke, Professor V. F. Weisskopf, Professor P. Demos, Professor A. G. Hill, Professor H. Joos, and Professor G. Weber, who made this collaboration possible. We also thank Professor A. Dar, Professor S. D. Drell, Professor E. Lohrmann, Professor G. Kramer, Professor B. Margolis, Professor L. Stodolsky, Professor J. S. Trefil, Dr. D. Lueke, Dr. P. Soeding, and Dr. H. Spitzer for interesting comments. We are grateful to Dr. Lublow, Mr. Kumpfert, Miss Ingrid Schulz, and Mr. Peter Berges for technical assistance.

¹For previous references on this reaction see Cambridge Bubble Chamber Collaboration, Phys. Rev. 146,

994 (1966), and 163, 1510 (1967); J. Ballam *et al.*, Phys. Rev. Letters 21, 1541, 1544 (1968); L. J. Lanza *et al.*, Phys. Rev. 166, 1365 (1968), H. Blechschmidt *et al.*, Nuovo Cimento 52A, 1348 (1967); W. G. Jones *et al.*, Phys. Rev. Letters 21, 586 (1969); Aachen-Berlin-Bonn-Hamburg-Heidelberg-München Collaboration, Phys. Rev. 175, 1669 (1968), and Phys. Letters 27B, 54 (1968); Y. Eisenberg *et al.*, Phys. Rev. Letters 22, 669 (1969); M. Davier *et al.*, Phys. Rev. Letters 21, 841 (1968), and Phys. Letters 28B, 619 (1969).

²G. McClellan, N. Mistry, P. Mostek, H. Ogren, A. Silverman, J. Swartz, R. Talman, K. Gottfried, and A. Lebedev, Phys. Rev. Letters 22, 374 (1969).

³J. G. Asbury *et al.*, Phys. Rev. 161, 1344 (1967).

⁴M. J. Longo and B. J. Moyer, Phys. Rev. 125, 701 (1962).

⁵M. N. Focacci and G. Giacomelli, CERN Report No. 66-18 (unpublished).

⁶By collecting the data only at forward angles ($\langle \theta_{\pi\pi} \rangle < 1^\circ$) with an average $t \approx 0.01$ (GeV/ c)², the effects of the t variable and the decay angular distribution are small. These features have already been measured (Ref. 1) and have been included in the calculation of the cross sections.

⁷P. Soeding, Phys. Letters 19, 702 (1965).

⁸J. D. Jackson, Nuovo Cimento 34, 1644 (1964).

⁹For the use of the term $(m_p/m)^4$ in the Breit-Wigner formula, see M. Ross and L. Stodolsky, Phys. Rev. 149, 1172 (1966); also, G. Kramer and J. L. Uretsky, (unpublished).

¹⁰F. James and M. Ross, CERN 6600 Computer Program Library Long Write-Up 67/623/1 (unpublished).

¹¹In obtaining $d\sigma/dt|_{t=0}$ from $d^2\sigma/d\Omega dm$ the normalization uncertainty of $\pm 10\%$, due to the spectrum functions used, is not shown in Fig. 2.

¹²S. C. C. Ting, in Proceedings of the Fourteenth International Conference on High Energy Physics, Vienna, Austria, 1968 (CERN Scientific Information Service, Geneva, Switzerland, 1968).